ELUCIDATING THE ROLE OF FOXJ3 IN REGULATING THE EXPRESSION OF SUPER ENHANCER ASSOCIATED KLF6 IN KIDNEY CANCER CELLS

CHE MUHAMMAD FARHAN BIN CHE ABDULLAH

FACULTY OF SCIENCE
UNIVERSITI MALAYA
KUALA LUMPUR

2022

ELUCIDATING THE ROLE OF FOXJ3 IN REGULATING THE EXPRESSION OF SUPER ENHANCER ASSOCIATED KLF6 IN KIDNEY CANCER CELLS

CHE MUHAMMAD FARHAN BIN CHE ABDULLAH

DISSERTATION SUBMITTED IN PARTIAL FULFILMENT OF THE REQUIREMENTS FOR THE DEGREE OF MASTER OF SCIENCE

INSTITUTE OF BIOLOGICAL SCIENCES
FACULTY OF SCIENCE
UNIVERSITI MALAYA
KUALA LUMPUR

2022

UNIVERSITI MALAYA

ORIGINAL LITERARY WORK DECLARATION

Name of Candidate: **CHE MUHAMMAD FARHAN BIN CHE ABDULLAH**

Matric No: **17043326/2**

Name of Degree: **MASTER OF SCIENCE (BIOTECHNOLOGY)**

Title of Dissertation ("this Work"):

ELUCIDATING THE ROLE OF FOXJ3 IN REGULATING THE EXPRESSION OF SUPER ENHANCER ASSOCIATED KLF6 IN KIDNEY CANCER CELLS

Field of Study:

MOLECULAR BIOLOGY

I do solemnly and sincerely declare that:

(1) I am the sole author/writer of this Work;
(2) This Work is original;
(3) Any use of any work in which copyright exists was done by way of fair dealing and for permitted purposes and any excerpt or extract from, or reference to or reproduction of any copyright work has been disclosed expressly and sufficiently and the tile of the Work and its authorship have been acknowledged in this Work;
(4) I do not have any actual knowledge nor do I ought reasonably to know that the making of this work constitutes an infringement of any copyright work;
(5) I hereby assign all and every rights in the copyright to this Work to the University of Malaya ("UM"), who henceforth shall be owner of any copyright in this Work and that any reproduction or use in any form or by any means whatsoever is prohibited without the written consent of UM having been first had and obtained;
(6) I am fully aware that if in the course of making this Work I have infringed any copyright whether intentionally or otherwise, I may be subject to legal action or any other action as may be determined by UM.

Candidate's Signature Date: 22 AUGUST 2022

Subscribed and solemnly declared before,

Witness's Signature Date: 22 AUGUST 2022

Name:

Designation:

ELUCIDATING THE ROLE OF FOXJ3 IN REGULATING THE EXPRESSION OF SUPER ENHANCER ASSOCIATED KLF6 IN KIDNEY CANCER CELLS

ABSTRACT

Kidney cancer is one of the top ten most diagnosed cancers worldwide. Of that, clear cell renal cell carcinoma (ccRCC) accounts for 75% of kidney cancer and death cases. ccRCC is associated with a mutation in Von Hippel-Lindau (VHL) tumour suppressor genes that causes accumulation of hypoxia-inducible factor (HIF). The conventional strategy to treat kidney cancer has been to target angiogenesis formation genes such as vascular endothelial growth factor (*VEGF*) that are upregulated from the abundance of HIF. Another target for kidney cancer treatment is the mechanistic target of rapamycin (mTOR) pathway using mTOR inhibitors. However, the treatments remain ineffective especially for patients with later stage cancers. Alternative therapeutic strategy for kidney cancers is to look at its transcriptional machinery. A super enhancer associated gene, Krüppel-like factor 6 (*KLF6*) has been identified as an important regulator in maintaining kidney cancer cell growth and fitness. The transcription factors (TFs) that bind to the super enhancer (SE) region near *KLF6* has yet to be fully identified. Preliminary DNA binding motif analysis has shown the transcription factor forkhead box J3 (*FOXJ3*) to be one of the TFs that bind to this SE region. This project had designed a CRISPR interference (CRISPRi) system targeting *FOXJ3* in kidney cancer cell line, 786-M1A that successfully showed a reduction of *FOXJ3* expression. This in turn leads to a reduction of *KLF6* expression making *FOXJ3* as one of the transcriptional machineries for *KLF6*. The relationship between *FOXJ3* and *KLF6* provides the data for completing the picture of the super enhancer assembly that drive *KLF6* expression.

Keywords: clear cell renal cell carcinoma, super enhancers, Krüppel-like factor 6, forkhead box J3, CRISPR interference

ELUCIDATING THE ROLE OF FOXJ3 IN REGULATING THE EXPRESSION OF SUPER ENHANCER ASSOCIATED KLF6 IN KIDNEY CANCER CELLS

ABSTRAK

Kanser buah pinggang adalah salah satu daripada sepuluh kanser yang paling kerap didiagnosis di seluruh dunia. Daripada jumlah itu, *clear cell renal cell carcinoma* (ccRCC) menyumbang sebanyak 75% kes kanser buah pinggang dan kematian. ccRCC telah dikaitkan dengan mutasi dalam gen penindas tumor *Von Hippel-Lindau* (*VHL*) yang menyebabkan pengumpulan *hypoxia-inducible factor* (HIF). Strategi biasa yang digunakan untuk merawat kanser buah pinggang adalah dengan menghalang pembentukan angiogenesis dengan menyasarkan gen yang teraktif disebabkan HIF yang banyak seperti *vascular endothelial growth factor* (*VEGF*). Salah satu lagi sasaran untuk rawatan kanser buah pinggang ialah *mechanistic target of rapamycin* (mTOR) menggunakan perencat mTOR. Walau bagaimanapun, rawatan-rawatan ini masih tidak berkesan terutamanya bagi pesakit kanser peringkat akhir. Maka dengan itu, strategi terapi alternatif untuk kanser buah pinggang adalah dengan menumpu pada proses transkripsi. Satu gen yang telah dikaitkan dengan *super enhancers* (SE) dalam kanser buah pinggang, *Krüppel-like factor 6* (*KLF6*) telah dikenal pasti sebagai komponen penting dalam mengekalkan pertumbuhan dan kecergasan sel kanser buah pinggang. *Transcription factor* (TF) yang berkait di kawasan SE berhampiran *KLF6* masih belum dikenal pasti sepenuhnya. Sebelum ini, analisa motif pengikat DNA telah menunjukkan *forkhead box J3* (FOXJ3) sebagai salah satu TF yang bergabung di kawasan SE ini. Projek ini telah mereka bentuk sistem *CRISPR interference* (CRISPRi) yang menyasarkan *FOXJ3* dalam sel kanser buah pinggang, 786-M1A yang mana telah berjaya menunjukkan pengurangan ekspresi *FOXJ3*. Ini seterusnya membawa kepada pengurangan ekspresi *KLF6* menjadikan *FOXJ3* sebagai salah satu jentera transkrip untuk *KLF6*. Hubungan

antara *FOXJ3* dan *KLF6* menyediakan data untuk melengkapkan gambar pemasangan SE yang memacu ekspresi *KLF6*.

Kata kunci: *clear cell renal cell carcinoma, super enhancers, Krüppel-like factor 6, forkhead box J3, CRISPR interference*

ACKNOWLEDGEMENTS

In the name of God, the Most Gracious, the Most Merciful. My greatest gratitude goes to Dr Saiful Effendi for his kindness and patience in teaching, mentoring, and supervising me during the research project. His critical thoughts, unconditional support, and willingness to share his in-depth knowledge has helped me to keep striving even when things were not working as I had hoped for. For this, I am enormously thankful for his genuine passion and dedication for science and for guiding aspiring researchers like myself.

I am also thankful to receive much help from Dr Nikman Adli regarding the technicalities of my candidature as a master's student. His constant reminders on deadlines, graduation milestones and advice put me on track to complete my research project without delay or extension.

My research project would also be impossible without the help of my fellow lab members, particularly Asmaa', Nurul Nadia and Mei Juan of whom many of our discussions led me to be more critical in my experiments and be more confident with facing any mistakes.

With all that said, it is not possible for me to undertake this postgraduate study without the support of my parents and family, and thus my deepest gratitude to them for believing in me in times when I would doubt myself. The COVID-19 pandemic was such a challenging time for many in the world including myself and having the backing of my family made it easier to complete this research project with a positive attitude and optimism.

TABLE OF CONTENTS

LIST OF FIGURES

LIST OF TABLES

LIST OF SYMBOLS AND ABBREVIATIONS

%	:	Percentage
°C	:	Degree Celcius
µg	:	Microgram
µL	:	Microlitre
µM	:	Micromolar
AnP	:	Antarctic Phosphatase
bp	:	Base pair
ccRCC	:	Clear cell renal cell carcinoma
cDNA	:	Complementary DNA
CDS	:	Coding sequence
ChIP	:	Chromatin immunoprecipitation
CRISPR	:	Clustered regularly interspaced short palindromic repeats
CRISPRi	:	CRISPR interference
dCas9	:	Dead Cas9
DMEM	:	Dulbecco′s Modified Eagle′s Medium
DNA	:	Deoxyribonucleic acid
dNTP	:	Deoxyribonucleoside triphosphate
E. coli	:	*Escherichia coli*
FBS	:	Fetal bovine serum
FOXJ3	:	Forkhead Box J3
g	:	Relative centrifugal force
H3K27ac	:	Histone H3 lysine 27 acetylation
HEK	:	Human embryonic kidney
HIF	:	Hypoxia-inducible factor

HIF2a	:	Hypoxia-inducible factor 2-alpha
KLF6	:	Krüppel-like factor 6
KRAB	:	Krüppel associated box
LB	:	Luria broth
MEF2C	:	Myocyte-specific enhancer factor 2C
MEME	:	Multiple expectation maximizations for motif elicitation
mL	:	Millilitre
mTOR	:	Mammalian target of rapamycin
NEB	:	New England Biolabs
ng	:	Nanogram
nm	:	Nanometre
Oligo-dT	:	Oligo deoxythymidine
PAM	:	Protospacer adjacent motif
PDGFB	:	Platelet-derived growth factor subunit B
qPCR	:	Quantitative polymerase chain reaction
RCC	:	Renal cell carcinoma
RE	:	Restriction enzymes
RNA	:	Ribonucleic acid
RNAse	:	Ribonuclease
rpm	:	Revolutions per minute
RPMI	:	Roswell Park Memorial Institute
Seq	:	Sequencing
sgRNA	:	Single guide RNA
TAE	:	Tris acetate-EDTA
U2OS	:	Human bone osteosarcoma epithelial cells
V	:	Voltage

VEGF	:	Vascular endothelial growth factor
VHL	:	Von Hippel-Lindau

CHAPTER 1: INTRODUCTION

1.1 Introduction

Kidney cancer, or renal cell carcinoma (RCC) is one of the top ten most common cancers diagnosed worldwide (Choueiri et al., 2021; Siegel et al., 2018). Of that, clear cell renal cell carcinoma (ccRCC) is the most common subtype of RCC to the account of 75% of all cases and encompasses for the majority of deaths for kidney cancer (Hsieh et al., 2017). ccRCC is associated with mutations in von-Hippel Lindau (*VHL*) tumour suppressor gene (Clark et al., 2019), which causes an accumulation of hypoxia-inducible factor alpha (HIFa) in the cells that activates many hypoxia-associated genes, including vascular endothelial growth factor (*VEGF*) gene (Choueiri & Motzer, 2017). *VEGF* is responsible for angiogenesis along with several other genes, and thus one of the treatment strategies for ccRCC is to target *VEGF* or its receptors (Choueiri & Motzer, 2017). Another therapeutic target for ccRCC treatment is the mechanistic target of rapamycin (mTOR) pathway through the use of mTOR inhibitors such as Everolimus and Temsirolimus (Choueiri & Motzer, 2017). mTOR pathway is hyperactivated in ccRCC (Pantuck et al., 2007; Robb et al., 2007) with genetic analyses have identified key mutations in the mTOR signalling cascade (Cancer Genome Atlas Research Network, 2013), all of which led to increased cell growth and division (Sabatini, 2006) making mTOR pathway a clinically relevant target in ccRCC. However, with varied treatment response and incomplete understanding of mechanisms underlying ccRCC pathogenesis, most patients receiving the treatments eventually progress to end-stage cancer (Motzer et al., 2014).

1.2 Problem Statement

As described, current treatment strategies for ccRCC remain ineffective. Therefore, there is a clear need for a novel therapeutic target and strategy to complement current ccRCC treatments. One of the strategies is to look at transcriptional regulators that govern the cancer cells growth and progression. Previous studies on transcriptional regulators in ccRCC have identified a super enhancer associated gene, Krüppel-like factor 6 (*KLF6*) gene that encodes for a zinc finger DNA-binding transcription factor (Syafruddin et al., 2019). *KLF6* have been shown to regulate the expression of several lipid homeostasis genes as well as platelet derived growth factor subunit B (*PDGFB*), an agonist of the mTOR pathway that promotes ccRCC growth (Syafruddin et al., 2019). Although *KLF6* activity is well established, the mechanism that regulate its expression is still not well understood, in particular the activity of super enhancers that affect *KLF6* expression. Syafruddin et al. (2019) has identified hypoxia-inducible factor (HIF) alpha as one of the transcription factors that act through binding at *KLF6* super enhancer region (Syafruddin et al., 2019). Preliminary DNA motif discovery analysis suggested forkhead box J3 (*FOXJ3*) as another potential transcription factor that work through this super enhancer region (Syafruddin, 2019). This research project thus aims to fill the gap by identifying one of the transcription factors that regulate *KLF6*, namely *FOXJ3*. By providing more understanding on how *KLF6* is regulated, it is hoped that a novel therapeutic strategy and target can be subsequently developed.

1.3 Research Aim

To determine whether *FOXJ3* regulates the expression of *KLF6* in kidney cancer cells.

1.4 Research Objectives

I. To construct a CRISPR interference system (CRISPRi) targeting *FOXJ3* expression in kidney cancer cells.

II. To select the positively transduced kidney cancer cells that carry the *FOXJ3*-targeting CRISPRi components from lentiviral transduction.

III. To assess the efficiency of CRISPRi-mediated *FOXJ3* repression in the transduced kidney cancer cells using quantitative real-time polymerase chain reaction (qPCR).

IV. To determine *KLF6* expression level upon *FOXJ3* targeting in the transduced kidney cancer cells using quantitative real-time polymerase chain reaction (qPCR).

CHAPTER 2: LITERATURE REVIEW

2.1 Super Enhancers

Transcription begins when RNA polymerase binds to promoters. The process is typically regulated by transcription factors that bind to specific DNA sequences to recruit the transcription machinery components (Tang et al., 2020). DNA sequences that contain the transcription factors binding sites are called “enhancers”, where they increase gene expression independent of distance, location and orientation to their target genes (Tang et al., 2020). “Super enhancers” on the other hand are clusters and collections of transcriptional enhancers that drive gene expression and determine cell identity (Hnisz et al., 2013; Sengupta & George, 2017). Notably, super enhancers have been shown to be important drivers in maintaining cancer cells identity (Hnisz et al., 2013; Thandapani, 2019) and cancer development (Tang et al., 2020) through transcriptional regulation of oncogenes (Sengupta & George, 2017). Super enhancers promote oncogenic transcription through two broad ways, first through genetic changes that affect the core super enhancer element which in turn lead to activation or repression of nearby target genes (Krijger & de Laat, 2016; Spielmann et al., 2018; Thandapani, 2019). Secondly, through genetic variations that cause changes in the three-dimensional configuration of the genome by altering the chromatin organization and form super-enhancer promoter looping leading to oncogene activation (Furlong & Levine, 2018; Spielmann et al., 2018; Thandapani, 2019). This all lead to cancer cells becoming highly addicted to oncogenic transcription of super-enhancer driven genes for proliferation and survival (Sengupta & George, 2017). This oncogenic addiction offers a viable option for therapeutic targeting in cancer cells by focusing on super-enhancers and their components (Sengupta & George, 2017).

Super enhancers-associated genes are also more sensitive to perturbation as compared to genes regulated by typical enhancers, therefore targeted inhibition of key transcription factor within the super enhancer assembly can hinder tumour viability and growth (Sengupta & George, 2017). For example, a study by Whyte et al. (2013) showed that knockdown of octamer-binding transcription factor 4 (*Oct4*) and Mediator, components that bind to super enhancers in pluripotent embryonic stem cells, caused more significant decrease in gene expression for super-enhancer-associated genes as compared to other genes (Whyte et al., 2013). Similar observation was seen in cancer cells where targeted inhibition of super-enhancer components supressed tumour progression, for example the small molecule inhibitor targeting super-enhancers, bromodomain and extraterminal protein inhibitor (BETi), has been shown to disrupt tumorigenic programs by inhibiting oncogenic transcription driven by super-enhancers (Thandapani, 2019). Early studies done by Delmore et al. (2011) and Zuber et al. (2011) showed BETi inhibited tumour progression in acute myeloid leukemia and multiple myeloma where MYC levels and its downstream transcriptional programs were suppressed (Delmore et al., 2011; Zuber et al., 2011). Often, super enhancers integrate diverse oncogenic signalling pathways in regulating gene expression, thus targeted inhibition of the key transcriptional regulators within the super enhancer assembly can hinder tumour viability and growth (Sengupta & George, 2017).

2.2 Krüppel-like Factor 6 (*KLF6*)

Previous study of super enhancers in ccRCC have discovered a super enhancer upstream of *KLF6*, which regulates lipid homeostasis (Syafruddin et al., 2019). *KLF6* belongs to the Krüppel-like factor (KLF) family, a DNA-binding transcription factor with multiple isoforms that regulate various pathways in cellular metabolism and mechanisms (Pollak et al., 2018). The characteristic feature of KLF family is the presence of three

Krüppel-like zinc fingers that bind to GC-rich regions of DNA and CACCC elements to regulate transcription (Pearson et al., 2008). The KLF members can act as either transcriptional activator or repressor with important roles in various disease pathogenesis (Pollak et al., 2018). KLF have context-dependent functions with different roles in normal and cancer cells, in different cancer stages and in different cancer types (Tetreault et al., 2013). *KLF6* is widely expressed in normal tissues (Pearson et al., 2008) with loss of function resulted in embryonic lethal in *Klf6* knockout mice (Matsumoto et al., 2006). Expression and activity of *KLF6* is altered in many human cancers from the wild-type *KLF6* that commonly inhibits proliferation and causes cell cycle arrest (Tetreault et al., 2013), with some cancer cells exhibit increased *KLF6* expression that promote proliferation and tumorigenesis (DiFeo et al., 2009). This includes prostate, lung, ovarian and kidney cancers among others (DiFeo et al., 2009; Tetreault et al., 2013).

Previous work by Syafruddin et al. (2019) has demonstrated that *KLF6* is upregulated in ccRCC than other cancer types and normal kidney tissues (Syafruddin et al., 2019). The association of *KLF6* with super enhancer in ccRCC was also determined by high histone H3 lysine 27 acetylation (H3K27ac) signal that is upstream to the *KLF6* locus (Syafruddin et al., 2019), where H3K27ac indicates active gene regulatory elements, specifically super enhancers (Roadmap Epigenomics Consortium et al., 2015; The ENCODE Project Consortium et al., 2012). p300 chromatin immunoprecipitation sequencing (ChIP-seq) data at the super enhancer H3K27ac signal showed several distinct p300 peaks known to be the transcription factor binding sites (**Figure 2.1**) (Syafruddin et al., 2019). DNA motif discovery analysis of one of the peaks revealed the presence of *FOXJ3* binding motif (Syafruddin, 2019), suggesting that *FOXJ3* is one of the transcription factors that drives *KLF6* expression through binding at the super enhancer

region. Empirical test is thus needed to confirm this hypothesis and is the basis for this research project.

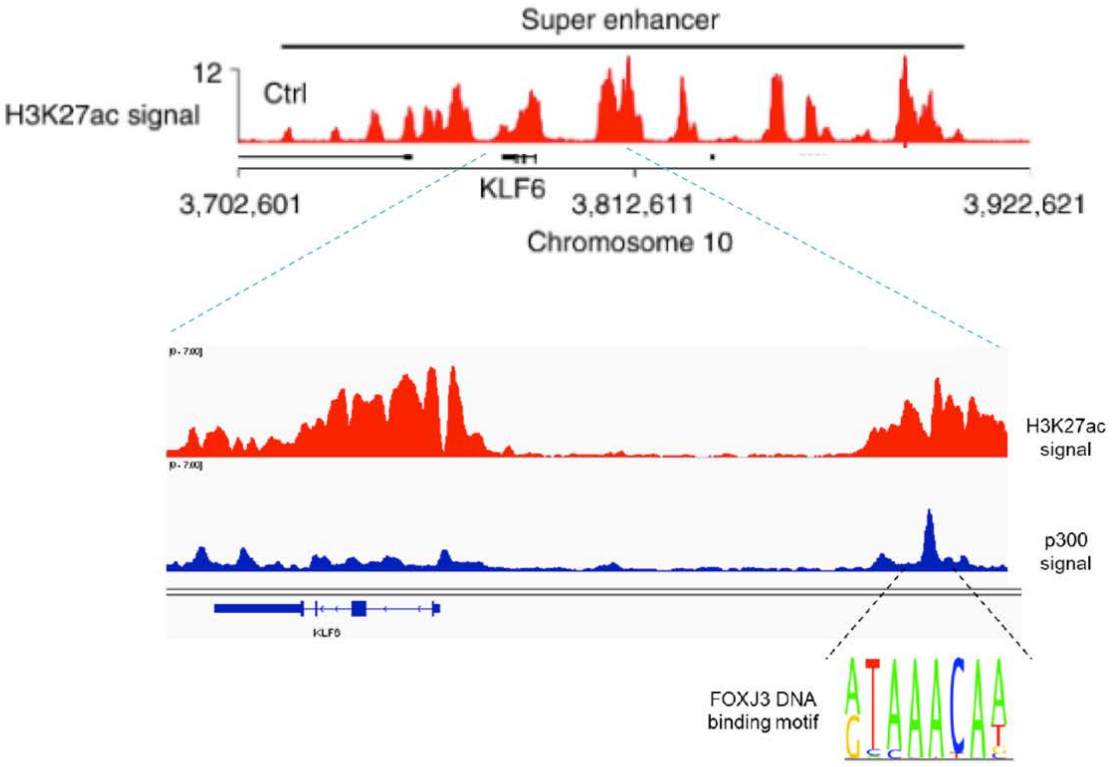

Figure 2.1: H3K27ac ChIP-seq signal at *KLF6* locus. Several peaks are shown with one of the nearest peaks to *KLF6* shows the presence of *FOXJ3* DNA binding motif. (Copyright permission from Syafruddin et al. (2019) and Syafruddin (2019))

2.3 Forkhead Box J3 (*FOXJ3*)

FOXJ3 belongs to the forkhead box (FOX) transcription factor family that typically interacts with chromatin and the transcription machinery (Carlsson & Mahlapuu, 2002). Forkhead box proteins mainly act as transcriptional activators and are key players in cell development and metabolism (Carlsson & Mahlapuu, 2002). *FOXJ3* was first described by Landgren & Carlson (2004) where *Foxj3* was shown to be expressed in neuroectoderm, neural crest and myotome in mice (Landgren & Carlsson, 2004). This suggests a functional role in the development of skeletal muscle as well as peripheral and central nervous system (Landgren & Carlsson, 2004). Studies on *Foxj3* mutant mice

exhibited impaired skeletal muscle contractile function and muscle regeneration; with myogenic progenitor cells have perturbed cell cycle kinetics (Alexander et al., 2010). *Foxj3* is also shown to work as transcriptional activator of myocyte-specific enhancer factor 2C (*Mef2c*) gene in regulating myofiber identity and muscle regeneration in mice (Alexander et al., 2010). Studies of human *FOXJ3* on the other hand shows a functional role in cell cycle control where knockdown of *FOXJ3* gene resulted in decreased cell proliferation rate (Grant et al., 2012). Subsequent analysis of genes regulated by *FOXJ3* in the same study revealed that it regulates a network of zinc finger proteins (Grant et al., 2012). In terms of disease pathogenesis, *FOXJ3* polymorphisms are shown to be associated with rheumatoid arthritis (Ban et al., 2013), and in human lung cancer, miR-517a-3p microRNA accelerates cell proliferation and invasion by inhibiting *FOXJ3* expression (Jin et al., 2014). Another microRNA, miR-425-5p is shown to regulate *FOXJ3* expression in prostate cancer (Zhang, Su, Li, & Guo, 2019) and glioblastoma (Rocha et al., 2020). In kidney cancer, The Cancer Genome Atlas (TCGA) data shows that high expression of *FOXJ3* is associated with poorer prognosis (Habuka et al., 2014; Uhlen et al., 2017; Human Protein Atlas proteinatlas.org), with screening of FOX family genes in ccRCC by Jia et al. (2018) showed the value of 0.96 hazard ratio for *FOXJ3* (Jia et al., 2018). No studies however were found to focus on the mechanism and target of *FOXJ3* in ccRCC to date.

CHAPTER 3: METHODOLOGY

3.1 To construct a CRISPR interference (CRISPRi) system targeting *FOXJ3* expression in kidney cancer cells.

3.1.1 sgRNA design using CRISPR design tool

The single guide RNA (sgRNA) that was used to target *FOXJ3* in kidney cancer cells was designed by using Broad Institute sgRNA design tool, CRISPick (https://portals.broadinstitute.org/gppx/crispick/public). From the online CRISPR design tool, five possible sgRNAs targeting the *FOXJ3* sequences were reported (**Table 3.1**).

Table 3.1: Possible sgRNAs generated from CRISPick

No.	Orientation	sgRNA Sequence (5'-3')	PAM Sequence
1	antisense	GTGCCTACTGCGAGCGGTCG	AGG
2	antisense	GCCCCGAGCAGCCCCGAGAG	CGG
3	antisense	CCGAGCAGCCCCGAGAGCGG	CGG
4	sense	TGCTGCCGCCGCCGCTCTCG	GGG
5	sense	GCCGCTCTCGGGGCTGCTCG	GGG

The target sites for the sgRNAs listed in **Table 3.1** within the *FOXJ3* cDNA were visualized using SnapGene Viewer (**Figure 3.1**).

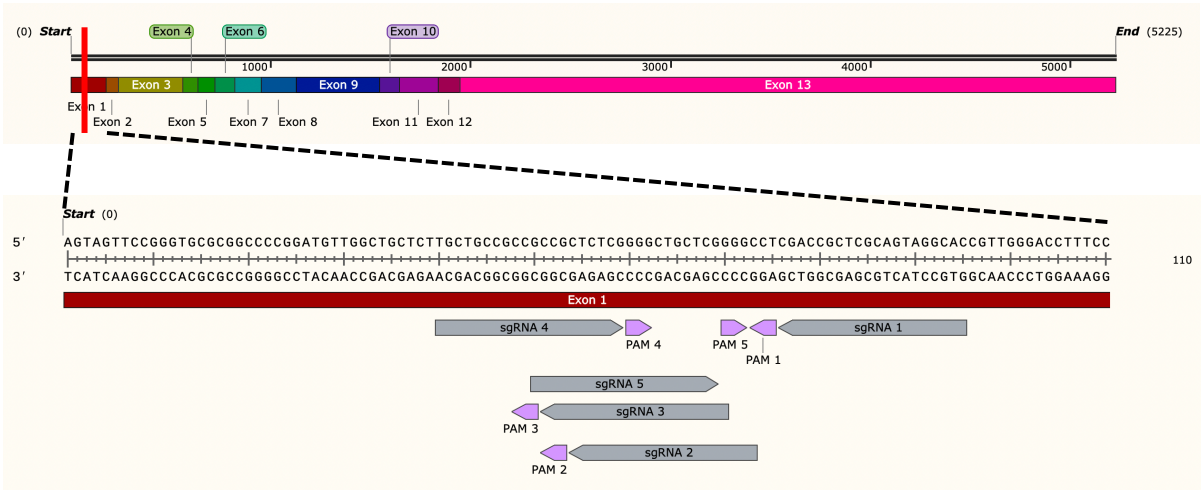

Figure 3.1: Top: *FOXJ3* cDNA with 13 exons. Bottom: The five possible sgRNAs target sites for repressing FOXJ3 using the CIRSPRi system. All target sites were located at Exon 1 near start codon. PAM = Protospacer adjacent motif.

As only one sgRNA could be chosen due to limited resources, sgRNA 2 was selected for the *FOXJ3* CRISPRi targeting because the region targeted by this sgRNA 2 was also bound by two other sgRNAs, sgRNA 3 and sgRNA 5, as shown in **Figure 3.1**. This was to ensure a higher chance of repression from the designed sgRNA, thus selecting sgRNA within a region with multiple possibilities would be a safe choice given the financial limitations. The selected sgRNA 2 was henceforth designated as iFOXJ3 (**Figure 3.2**).

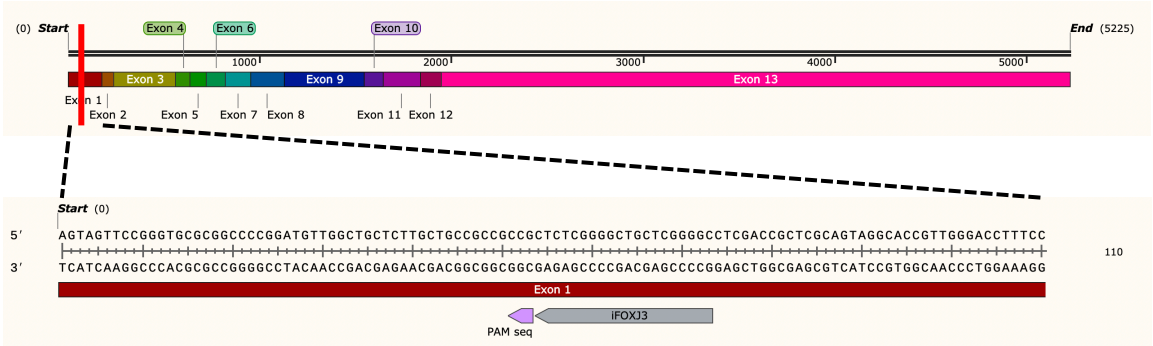

Figure 3.2: **CRISPRi *FOXJ3* targeting. The sgRNA chosen from the online design tool, iFOXJ3 (sgRNA 2), targeted the region within *FOXJ3* Exon 1.**

For CRISPRi targeting, dead Cas9 (dCas9) fused with Krüppel-associated box (KRAB) repression domain was employed. The dCas9-KRAB would be recruited to the iFOXJ3 target site and subsequently mediated the repression of *FOXJ3* expression. The iFOXJ3 construct were then generated by designing and purchasing the sense and antisense strands separately. Moreover, *BbsI* restriction enzyme overhangs were incorporated into the 5' and 3' end of each strand (**Table 3.2**). These *BbsI* restriction overhangs would be utilized to insert the iFOXJ3 sgRNA into an expression vector, which will be discussed in the sections below.

Table 3.2: iFOXJ3 sense and anti-sense strands construct, with *BbsI* restriction enzyme overhangs underlined.

Oligo Name	sgRNA Sequence
iFOXJ3 sense strand	5' CACCG GCC CCG AGC AGC CCC GAG AG GT 3'
iFOXJ3 reverse strand	5' TAAAAC CTC TCG GGG CTG CTC GGG GC C 3'

3.1.2 iFOXJ3 sense and antisense strands annealing and phosphorylation

The purchased iFOXJ3 constructs were received in lyophilized form from Integrated DNA Technologies, Inc. (IDT), Singapore. The lyophilized iFOXJ3 sense and anti-sense strands were first resuspended in RNase free water to achieve final concentration of 100 µM. These sense and anti-sense constructs were then annealed and phosphorylated using T4 Polynucleotide Kinase (NEB #M0201) and T4 DNA Ligase Buffer (NEB #B020S). Briefly, 1 µL of the resuspended strands were added to 1 µL of T4 Polynucleotide Kinase and 1 µL of T4 DNA Ligase Buffer. 6 µL of water was added to make the final reaction volume of 10 µL. The mixture was incubated at 37°C for 30 minutes, then heat inactivated at 95°C for 5 minutes and ramped down to 25°C at the rate of 5°C per minute. The

ramping down was performed to allow the iFOXJ3 sense and antisense sgRNA strands to anneal at their optimum temperatures. T100 thermal cycler (Bio-Rad) was used for the incubation with the settings.

3.1.3 sgRNA expression plasmid digestion with *BbsI* restriction enzyme

The sgRNA expression plasmid pKLV-U6gRNA(BbsI)-PGKpuro2ABFP was a gift from Kosuke Yusa (Addgene #50946) (Koike-Yusa et al., 2014). The plasmid was modified to pKLV-U6gRNA(BbsI)-PGKhygro2ABFP made available from the supervisor's lab and was used as the expression plasmid for the sgRNA (Syafruddin et al., 2019). The expression plasmid contained *BbsI* restriction enzyme sites, ampicillin resistance gene, and hygromycin resistance gene. The plasmid was first quantified using NanoDrop™ 2000 Spectrophotometer (Thermo Fisher Scientific). Then, 2 µg of the sgRNA expression plasmid was digested with *BbsI* restriction enzyme. Digestion reaction was set up with 2 µg of the plasmid, 20 units of high-fidelity *BbsI* restriction enzyme (NEB #R3539) and 1X of rCutSmart™ Buffer (NEB #B6004). Water was added to make 50 µL of total final volume reaction. The digestion reaction was incubated at 37°C for 2 hours, followed by heat-inactivation at 65°C for 20 minutes in T100 thermal cycler.

3.1.4 Antarctic Phosphatase (AnP) treatment

The *BbsI*-digested plasmid was then treated with 10 unit of Antarctic Phosphatase (NEB #M0289) and 1X of Antarctic Phosphatase Buffer (NEB #B0289). Water was added to make 60 µL of total final volume reaction. This AnP 5' dephosphorylation reaction was incubated at 37°C for 1 hour, followed by heat-inactivation at 70°C for 5 minutes in T100 thermal cycler.

3.1.5 Agarose gel electrophoresis of the digested sgRNA expression plasmid

The treated and digested sgRNA expression plasmid was separated using agarose gel electrophoresis. The agarose gel was first prepared with 30 mL of 1X tris acetate EDTA (TAE) buffer and 1% of agarose powder in a conical flask. The mixture was heated in a microwave under medium setting for 2 minutes. The mixture was then cooled under running water and periodically swirled before 3 µL of FloroSafe DNA Stain (1st BASE) was added. The gel was poured onto a casting tray with the comb fixed and let to cool for 30 minutes. Once the gel has solidified, the comb was removed, and the gel was put into the running tank. 1X TAE buffer was poured into the running tank until it covered the gel. 1X of Purple Loading Dye (NEB #B7024) was added to the digested plasmid before it was loaded into the well. 6 µL of 1 kb GeneRuler (Thermo Fisher Scientific #SM0311) was also loaded along with the sample. The gel was run at 100 V for 30 minutes before visualised using VILBER gel documentation system.

3.1.6 Gel purification

The separated sgRNA expression plasmid (**3.1.5**) was extracted and purified from the gel using QIAquick® Gel Extraction Kit (QIAGEN). First, the digested plasmid was cut from the agarose gel with a scalpel and weighed. 3 volumes of Buffer QG (solubilization and binding buffer) were added per 1 volume gel. The reaction was incubated at 55°C for 10 minutes while vortexed every 2 to 3 minutes to dissolve the gel. Once the gel had completely dissolved, 250 µL of isopropanol was added to the sample and mixed. The sample was then applied onto QIAquick column and centrifuged at 17,900 x *g* for 1 minute with the resulting flow-through discarded. Then, another 500 µL of Buffer QG was added to the column and centrifuged at 17,900 x *g* for 1 minute. Next, 750 µL of Buffer PE (wash buffer) was added to the column and centrifuged at 17,900 x *g* for 1 minute. The column was centrifuged once more to remove any remaining wash buffer.

The column was then transferred to a new 1.5 mL microcentrifuge tube. The plasmid was eluted with 30 µL of Buffer EB (elution buffer) by adding the buffer to the centre of the column and centrifuged at 17,900 x *g* for 1 minute. The purified plasmid was then quantified using NanoDrop™ 2000 Spectrophotometer.

3.1.7 Ligation of the iFOXJ3 into the sgRNA expression plasmid

Once the digested and phosphatase-treated plasmid has been purified and quantified, the annealed sgRNA from **3.1.2** was ligated into the plasmid. The annealed sgRNA was first diluted in RNase-free water to 1:200. Ligation reaction was then set up with 50 ng of the digested plasmid, 5 µL of the diluted and annealed sgRNA, 1 µL of T4 DNA Ligase (NEB #M0202), 2 µL of T4 Ligase Buffer (NEB #B0202), and water for the final volume of 20 µL. A negative control ligation reaction was also prepared by replacing the sgRNA with water. The reaction was performed with overnight incubation at 16°C (~18 hours) followed by heat-inactivation at 65°C for 10 minutes in T100 thermal cycler. **Figure 3.3** illustrates the cloning strategy that was carried out through methodology **3.1.1** to **3.1.7**.

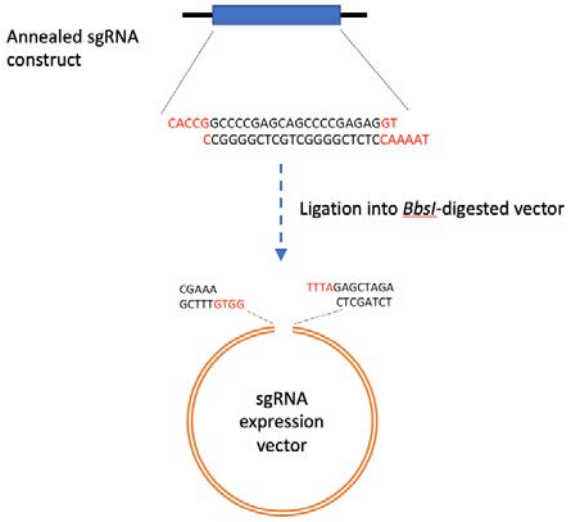

Figure 3.3: Cloning strategy of iFOXJ3 construct into pKLV-U6gRNA(BbsI)-PGKhygro2ABFP sgRNA expression plasmid.

3.1.8 Bacterial transformation

The ligated plasmid and the negative control reaction were then transformed into chemically competent *Escherichia coli* (DH5α). These chemically competent *E.* coli was previously generated in-house by the supervisor's lab group using calcium chloride treatment. Vials containing 100 µL of *E. coli* were first thawed on ice. Then, 20 µL of the ligated plasmid was added into the tube and mixed gently by flicking 3 to 4 times. The bacteria were then incubated on ice for 30 minutes, then heat shocked at 42°C for 30 seconds and returned on ice for another 5 minutes. 300 µL of pre-warmed Luria broth (LB) was added to the bacteria, then incubated at 37°C while shaking (250 rpm) in an incubator shaker (New Brunswick Scientific) for 1 hour. Then, 400 µL of the bacteria was plated on LB agar plate supplemented with 100 µg/mL of ampicillin. The bacteria plate was then incubated overnight at 37°C in an incubator (Memmert). On the following day, bacterial colonies were picked and cultured in 3 mL of LB broth supplemented with 100 µg/mL of ampicillin. The picked colony was then incubated at 37°C while shaking (250 rpm) in an incubator shaker for 16 to 18 hours.

3.1.9 Plasmid extraction

The plasmids from the picked bacterial colonies were extracted using Monarch® Plasmid Miniprep kit (NEB). Firstly, 3 mL of the bacteria culture was pelleted in a 1.5 mL microcentrifuge tube by centrifugation at 16,000 x *g* for 1 minute. This was performed by transferring 1.5 mL of the bacteria culture and centrifuged with the supernatant removed twice. The resulting pellet was then resuspended with 200 µL of Plasmid Resuspension Buffer (B1) by pipetting up and down. Once there were no visible clumps, 200 µL of Plasmid Lysis Buffer (B2) was added into the tube and gently inverted several times, then incubated at room temperature for 1 minute. Next, 400 µL of Plasmid Neutralization Buffer (B3) was added and gently inverted a few times until the sample

was neutralized, indicated when the sample was uniformly yellow and formed precipitate. The lysate was then centrifuged at 16,000 x *g* for 5 minutes. The supernatant was transferred to a spin column and centrifuged at 16,000 x *g* for 1 minute. Then, 200 µL of Wash Buffer 1 was added and centrifuged at 16,000 x *g* for 1 minute. Next, 400 µL of Wash Buffer 2 was added and centrifuged at 16,000 x *g* for 1 minute. The column was centrifuged again to remove residual wash buffer before transferring the column to a new 1.5 mL microcentrifuge tube. The plasmid was eluted by adding 30 µL of DNA Elution Buffer to the centre of the column and centrifuged at 16,000 x *g* for 1 minute. The extracted plasmid was then quantified with NanoDrop™ 2000 Spectrophotometer. The plasmid was then sent to 1st BASE for sequencing using Sanger sequencing with U6 forward primer to confirm the presence of sgRNA insert in the plasmid.

3.2 To select the positively transduced kidney cancer cells that carry the *FOXJ3*-targeting CRISPRi components from lentiviral transduction.

3.2.1 Culturing HEK293T cells for lentiviral production

Human embryonic kidney (HEK) 293T cells were used to produce lentiviral particles. The cells were plated in 6-wells plate at a density of 1 x 10^6 cells per well and cultured in Dulbecco's Modified Eagle Medium (DMEM), supplemented with 10% fetal bovine serum (FBS) and 1% penicillin and streptomycin (Pen-Strep). The cells were incubated overnight to approximately 70-80% confluency on the following day for lentiviral production.

3.2.2 Lentiviral production

The HEK293T cells were co-transfected with the packaging plasmid, psPAX2 (Addgene #12260), envelope plasmid, pMD2.G (Addgene #12259), and the iFOXJ3-

expressing plasmid (prepared in **3.1.9**). Transfection mix was prepared with 1.3 µg of psPAX plasmid, 0.5 µg of pMD2.G plasmid, 1.5 µg of iFOXJ3-expressing plasmid and serum-free media for the final volume of 200 µL. 15 µL of transfection reagent Attractene (QIAGEN #301005) was then added dropwise into the transfection mix and incubated at room temperature for 30 minutes. The HEK293T cells media was replenished with 1.7 mL fresh DMEM media. Then, the transfection mixture was added dropwise onto the prepared HEK293T cells. Thus, the total volume of cell media along with the transfection mix was approximately 2 mL. The HEK293T cells were then incubated for 48 to 72 hours before lentiviral particles were harvested. In addition, non-targeting control lentiviral particles were also produced by transfecting the HEK293T cells with plasmids carrying non-targeting sgRNA (hereinafter referred to sgNTC). The sgNTC plasmids were previously generated by Syafruddin (2019) through similar methodology described in the cloning of sgRNA into expression plasmid (**Table 3.3**).

Table 3.3: sgNTC sequence (Syafruddin, 2019)

Construct	sgRNA Sequence
sgNTC	5' GAGTGTCGTCGTTGCTCCTA 3'

3.2.3 Lentiviral particles harvest

The lentiviral particles were harvested 48-72 hours post-transfection. Media containing the lentiviral particles was collected and filtered through 5 mL syringe and 0.45 µM syringe filter. The filtrate was collected in cryovial tubes and stored in -80°C until cell transduction was ready. **Figure 3.4** illustrates the lentiviral production step.

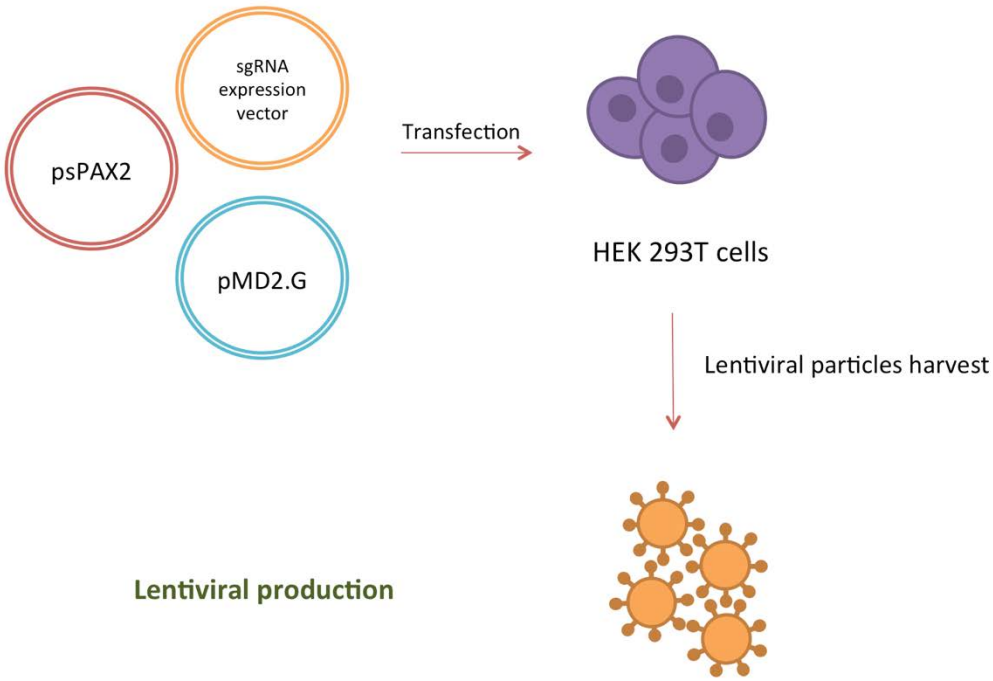

Figure 3.4: Lentiviral production and harvest. The virus was produced in HEK293T cells through transfection with psPAX2, pMD2.G, and the iFOXJ3 expressing plasmid. For control, sgNTC plasmid was used in place of iFOXJ3 expressing plasmid.

3.2.4 Culturing kidney cancer cells for lentiviral transduction

The clear cell renal cell carcinoma cell line used in this research was the 786-M1A cell line. This cell line was established from 786-O renal cell carcinoma cell line as its metastatic derivative (Vanharanta et al., 2012). 786-O cell line is the most used cell line and model for RCC-focused research due to its defective *VHL* expression and increased HIF2A and VEGF protein expression, which are the characteristics of ccRCC (Brodaczewska et al., 2016; Wolf et al., 2020). The 786-M1A cell line had also been engineered to stably express the dCas9-KRAB protein (786-M1A CRISPRi cells), made available from the supervisor's lab. The cells were plated in 6-well plate at a density of 3 x 10^5 cells per well and cultured in Roswell Park Memorial Institute Medium (RPMI-1640) supplemented with 10% FBS and 1% Pen-Strep. The cells were incubated

overnight until there were approximately 70-80% confluency on the following day for lentiviral particles transduction.

3.2.5 Lentiviral transduction of kidney cancer cells

To begin the transduction, 1.8 mL of fresh RPMI media was added to the 786-M1A CRISPRi cells. Next, transfection reagent Polybrene (Merck Millipore #TR-1003-G) was added into the media for final concentration of 8 μg/mL. The cell plate was swirled gently to mix. 200 μL of the harvested lentiviral particle was then added to the plated cells dropwise and mixed by swirling. Two plates of iFOXJ3 cells were cultured, together with one plate of sgNTC cells, as well as one plate untransduced cells with no lentiviral particles added as control. The cells were then incubated overnight. On the following day, the media was removed, and the cells were washed with 1x PBS once with fresh media added afterwards. Cells were then incubated for another 24 hours.

3.2.6 Antibiotic selection of positively transduced cells

After the cells have been transduced, the positively transduced cells were selected via antibiotic selection. As the plasmid pKLV-U6gRNA(BbsI)-PGKhygro2ABFP contained hygromycin resistance gene, the transduced 786-M1A CRISPRi cells was selected using hygromycin. The cell media was replaced with selection media supplemented with 900 μg/mL of hygromycin. The cells were maintained for 5 days. The surviving cells (positively transduced) were pooled and maintained for subsequent analysis. The cell colonies were not picked as CRISPRi were used to repress *FOXJ3* gene instead of a total knockout. Thus, expression of the gene-of-interest would still be present even if the cell colonies were picked. For this reason, cell pooling method was chosen.

3.2.7 Cell expansion

To ensure the cells were readily available for analysis, the transduced cells were expanded in a 6 cm dish. The media was removed, and the cells were washed with 1 mL of 1X PBS and removed afterwards. Then, 200 µL of trypsin was added to detach the cells from the plate and incubated for 6 minutes in 37°C incubator. 1 mL of fresh RPMI-1640 media supplemented with 10% FBS and 1% Pen-Strep was then added to the trypsinised cells and transferred to a 6 cm plate with 3 mL of media pre-added. The cells were then returned to the incubator and let to expand. When it reached 80-100% confluency, the cells were passaged to a 10 cm plate using similar method with slight increase of reagent volumes. The cells were then maintained in 10 cm plate with fresh media changed every 3 to 4 days.

3.3 To assess the efficiency of CRISPRi-mediated *FOXJ3* repression in the transduced kidney cancer cells using quantitative real-time polymerase chain reaction (qPCR).

3.3.1 Collecting the cells

Once the positively transduced cells have been selected, pooled, and maintained, the efficiency of CRISPRi targeting *FOXJ3* was assessed. The cells were pelleted at 80% confluency for subsequent analysis. In brief, cell media was removed, and the cells were washed with 4 mL of 1X PBS and removed afterwards. Then, 1 mL of trypsin was added to detach the cells from the plate and incubated for 6 minutes in 37°C incubator. 4 mL of RPMI-1640 media was added to the trypsinized cell and transferred to a 15 mL centrifuge tube. 500 µL of the cell was re-plated in a new 10 cm plate with 8 mL RPMI-1640 media pre-added to be maintained. The rest of the cells were centrifuged at 1,200 rpm for 3 minutes to produce cell pellet with the supernatant removed.

3.3.2 Total RNA extraction

Once the cell has been pelleted, total RNA was extracted by using TRIzol® reagent (Thermo Fisher Scientific). Firstly, the cell pellet was resuspended in 1 mL of 1X PBS and transferred to a 1.5 mL microcentrifuge tube. The tube was centrifuged at 1,200 x *g* for 5 minutes at 4°C. After supernatant was removed, 200 µL of TRIzol® reagent was added to the pellet and vigorously suspended to lyse the cells. The homogenized sample was incubated for 5 minutes at room temperature before adding 40 µL of chloroform. The tube was shaken vigorously by hand and incubated at room temperature for 2-3 minutes. The sample was then centrifuged at 12,000 x *g* for 15 minutes at 4°C to separate the mixture. The aqueous phase (top layer) was carefully removed without taking any of the interphase or organic layer and placed into a new 1.5 mL microcentrifuge tube. 100 µL of 100% isopropanol was then added to the aqueous phase to precipitate RNA and incubated at room temperature for 10 minutes. The mixture was then centrifuged at 12,000 x *g* for 10 minutes at 4°C. The supernatant was removed leaving only the RNA pellet. 200 µL of 75% ethanol was then added to the tube to wash the pellet. The sample was vortexed briefly and centrifuged at 7,500 x *g* for 5 minutes at 4°C. The supernatant was removed ensuring that only the pellet was left behind. The tube was briefly spun before removing residual ethanol to ensure high purity of RNA extracted. The sample was also air dried for 2-3 minutes before RNase-free water was added to solubilise the RNA pellet. The sample was then incubated at 55°C for 2-3 minutes. The yield and quality of the extracted RNA were determined using NanoDrop™ 2000 Spectrophotometer.

3.3.3 Complementary DNA (cDNA) synthesis

cDNA was synthesized from the extracted RNA using LunaScript® RT SuperMix Kit (NEB #E3010). The cDNA synthesis reaction was prepared with 2µL of LunaScript RT SuperMix (NEB #M3010), 500 ng of extracted RNA and nuclease-free water for final

volume of 10 µL. The supermix contained random hexamer and oligo-dT primers, RNase inhibitor, and reverse transcriptase. The reaction was incubated in T100 thermal cycler with primer annealing step done at 25°C for 2 minutes, then cDNA synthesis at 55°C for 10 minutes, followed by heat inactivation at 95°C for 1 minute.

3.3.4 Quantitative polymerase chain reaction (qPCR)

FOXJ3 expression was determined from the synthesized cDNA using qPCR. This was performed to determine the efficiency of the CRISPRi targeting system and measure *FOXJ3* expression in the CRISPRi-mediated repression 786-M1A cells. The qPCR was performed using Luna® Universal Probe qPCR Master Mix (NEB #M3004). The qPCR reaction mix was prepared with 2.5 µL of qPCR Master Mix, 0.25 µL of probe and 2 µL of diluted 1:10 cDNA. The Taqman probes used were *FOXJ3* (Hs00961536_m1) and beta-actin (*ACTB*) (Hs01060665_g1) from Thermo Fisher Scientific. *ACTB* was the most used reference gene for RCC research (Jung et al., 2007) and its use to measure changes of *FOXJ3* expression via qPCR had been previously employed (Simeoni et al., 2021). The master mix and Taqman probes were first mixed and transferred to an optical reaction qPCR 8-tubes strip in triplicate. Then the synthesized cDNA was added into the tubes. The qPCR tube strip was placed in CFX Real-Time PCR Detection System (Bio-Rad) with initial denaturation step at 95°C for 1 minute, then 40 cycles of denaturation at 95°C for 15 seconds and extension at 60°C for 30 seconds. The resulting amplification plots for the reactions were then analysed to determine *FOXJ3* gene expression.

3.3.5 Delta-delta C_t ($\Delta\Delta C_t$) analysis

The double delta C_t ($\Delta\Delta C_t$) approach was employed to analyse the qPCR data. This analysis measures the relative changes in the gene expression between two or many groups by normalizing to stable expression levels of reference genes (Livak &

Schmittgen, 2001). In this case, the relative change in *FOXJ3* expression between *FOXJ3*-targeted and control cells was determined. Briefly, *FOXJ3* and *ACTB* cycle threshold value (C_t) was averaged for the experimental condition (iFOXJ3) and control (sgNTC). The differences of the Ct values (ΔC_t) of the genes were then calculated in both conditions (Equation 3.1).

$$\Delta C_t = Avg.C_{t,FOXJ3} - Avg.C_{t,Actin} \quad (3.1)$$

Next, the double delta Ct value ($\Delta\Delta C_t$) was calculated by normalizing experimental ΔC_t to control ΔC_t (Equation 3.2 and 3.3).

$$iFOXJ3\ \Delta\Delta C_t = \Delta C_{t,iFOXJ3} - \Delta C_{t,sgNTC} \quad (3.2)$$

$$sgNTC\ \Delta\Delta C_t = \Delta C_{t,sgNTC} - \Delta C_{t,sgNTC} \quad (3.3)$$

Finally, the fold change in gene expression was calculated by using $2^{-\Delta\Delta Ct}$.

3.4 To determine *KLF6* expression level upon *FOXJ3* targeting in the transduced kidney cancer cells using quantitative real-time polymerase chain reaction (qPCR).

3.4.1 qPCR gene expression analysis

Once the efficiency of the CRISPRi *FOXJ3* targeting have been determined, the resulting effect of *FOXJ3* repression on *KLF6* expression level was measured. The *KLF6* expression level was determined using similar protocol for qPCR in **3.3.4** by probing for *KLF6* (Hs00810569_m1, Thermo Fisher Scientific) and was carried out at the same time.

The experiment was repeated two more times from pelleting cells in **3.3.1** to qPCR analysis in **3.3.5** to obtain three experimental repeats.

CHAPTER 4: RESULTS

4.1 Agarose gel electrophoresis

Agarose gel electrophoresis was used to separate and purify the *BbsI*-digested/Antarctic Phosphatase-treated pKLV-U6gRNA(BbsI)-PGKhygro2ABFP plasmid (**Figure 4.1a**). The gel image showed the plasmid in linear conformation. The size of the plasmid without insert was 8102 bp based on supplier's information (Addgene #50946). The presence of one linear band indicates that the plasmid was completely digested with *BbsI* restriction enzyme. Incomplete or partially digested plasmid would appear in the three conformations: linear, circle and supercoiled. For comparison, the undigested plasmid was run on a separate gel to illustrate the conformational difference of between digested and undigested plasmid (**Figure 4.1b)**

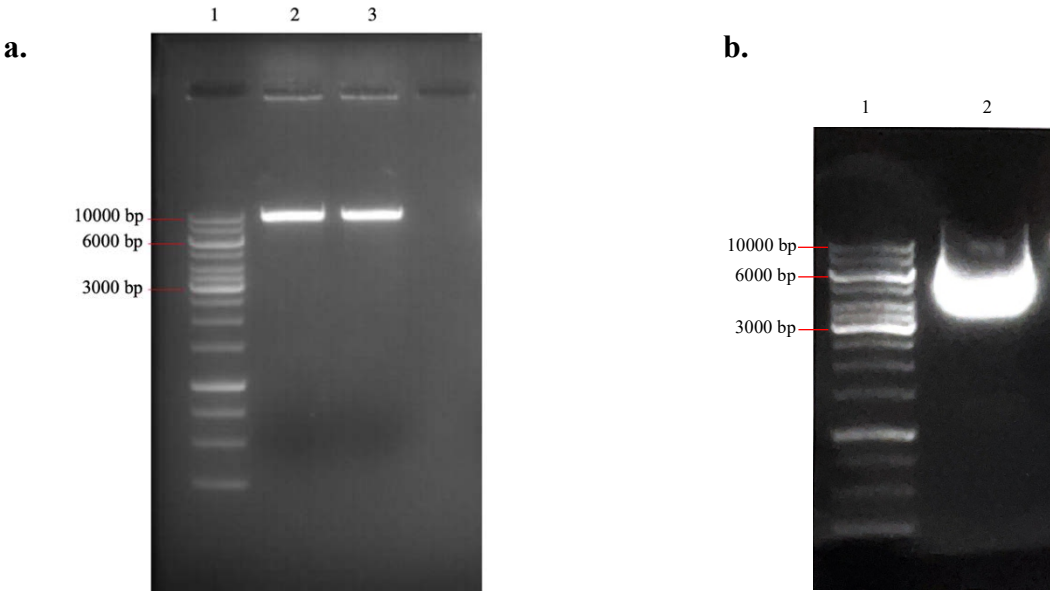

Figure 4.1: a) Agarose gel electrophoresis of *BbsI*-digested and Antarctic Phosphatase-treated pKLV-U6gRNA(BbsI)-PGKhygro2ABFP plasmid. Lane 1: 1 kb DNA Ladder; lanes 2-3: digested plasmids. b) Agarose gel electrophoresis of undigested pKLV-U6gRNA(BbsI)-PGKhygro2ABFP plasmid. Lane 1: 1 kb DNA Ladder; lane 2: undigested plasmid in supercoiled conformation.

4.2 Ampicillin-resistant *E. coli* from the bacterial transformation

The iFOXJ3-ligated and negative control sgRNA expression plasmids were transformed into chemically competent *E. coli* (DH5α) and plated onto LB + ampicillin plates. **Figure 4.2** shows the colonies of the *E. coli* transformed with iFOXJ3-ligated (left) and negative control sgRNA expression plasmids (right). The iFOXJ3 construct produced a good number of bacterial colonies because the plasmid was intact upon the iFOXJ3 ligation, resulting in the expression of ampicillin resistant gene. As expected, the negative control plate has significantly lower number of formed *E. coli* colonies, where only a few colonies were observed.

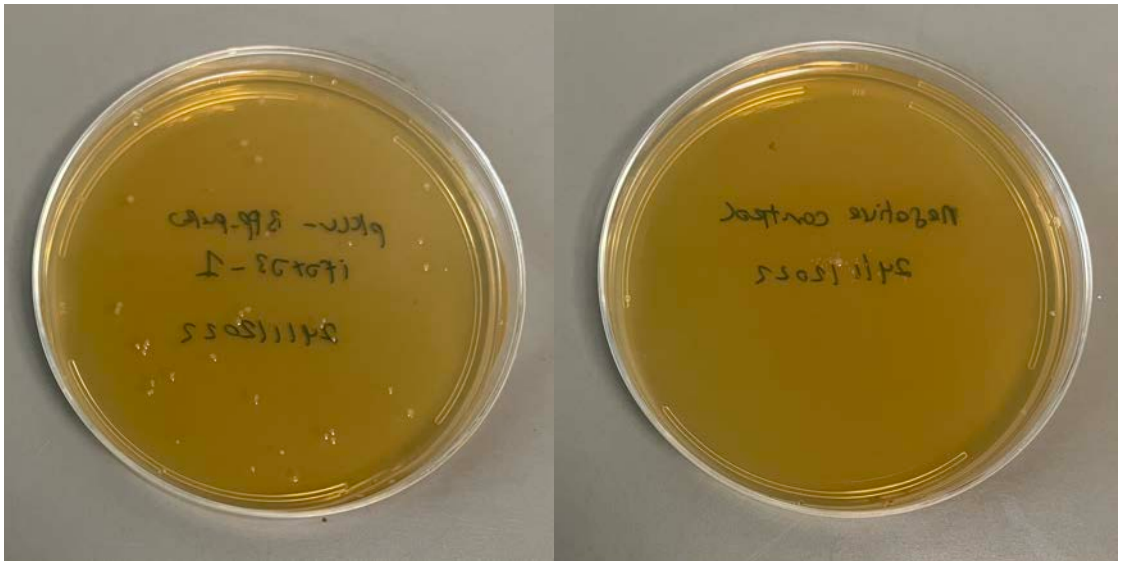

Figure 4.2: Colonies of the *E. coli* transformed with iFOXJ3-ligated (left) and negative control sgRNA expression plasmids (right). White dots on the plate indicate the bacterial colony.

4.3 Sanger sequencing of the plasmid extracted from bacterial colony

Several colonies were picked and cultured in LB broth for plasmid extraction. This extracted plasmid was used for lentiviral production and transduction into the cells to repress *FOXJ3* expression. Prior to performing the lentiviral production, the presence of

the ligated iFOXJ3 construct in the sgRNA expression plasmid was first verified via Sanger sequencing (1st BASE). The presence of the inserted iFOXJ3 construct, *GCCCCGAGCAGCCCCGAGAG*, was confirmed in the sgRNA expression plasmid (**Figure 4.3**).

a.

GGGGAGTGGGACTACGCGTTACTCGAGCCAAGGTCGGGCAGGAAGAGGGCCTA
TTTCCCATGATTCCTTCATATTTGCATATACGATACAAGGCTGTTAGAGAGAT
AATTAGAATTAATTTGACTGTAAACACAAAGATATTAGTACAAAATACGTGAC
GTAGAAAGTAATAATTTCTTGGGTAGTTTGCAGTTTTAAAATTATGTTTTAAA
ATGGACTATCATATGCTTACCGTAACTTGAAAGTATTTCGATTTCTTGGCTTT
ATATATCTTGTGGAAAGGACGAAACACCGGCCCCGAGCAGCCCCGAGAGGTTT
TAGAGCTAGAAATAGCAAGTTAAAATAAGGCTAGTCCGTTATCAACTTGAAAA
AGTGGCACCGAGTCGGTGCTTTTTTTGGATCCGGGTAGGGGAGGCGCTTTTCC
CAAGGCAGTCTGGAGCATGCGCTTTAGCAGCCCCGCTGGGCACTTGGCGCTAC
ACAAGTGGCCTCTGGCCTCGCACACATTCCACATCCACCGGTAGGCGCCAACC
GGCTCCGTTCTTTGGTGGCCCCTTCGCGCCACCTTCTACTCCTCCCCTAGTCA
GGAAGTTCCCCCCCGCCCCGCAGCTCGCGTCGTGCAGGACGTGACAAATGGAA
GTAGCACGTCTCACTAGTCTCGTGCAGATGGACAGCACCGCTGAGCAATGGAA
GCGGGTAGGCCTTTGGGGCAGCGGCCAATAGCAGCTTTGCTCCTTCGCTTTCT
GGGCTCAGAGGCTGGGAAGGGGTGGGTCCGGGGGCGGGCTCAGGGGCGGGCTC
AGGGGCGGGGCGGGCGCCCGAAGGTCCTCCGGAGGCCCGGCATTCTGCACGCT
TCAAAAGCGCACGTCTGCCGCGCTGTTCTCCTCTTCCTCATCTCCGGGCCTTT
CGACCTGGATCCCGCCACCATGAAAAAGCCTGAACTCACCGCGACGTCTGGCC
AGAAGTTTCTGATCGAAAAGTCCGAAGCGGCTCCGAACTGATGCATCTCCCGA
AGGGTAAAAACCCCTTGTTTTCCTTTCAATGTAGGAGGCTTGGGAATGCCCTC
GGAAAAATAATAGCCCATTGGTTACCACAAAACTTGCCATTTATCACCATTTT
CTAAGCCA

b.

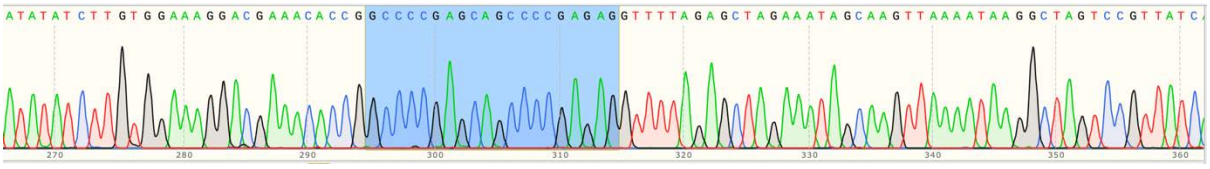

Figure 4.3: DNA sequence of plasmid extracted from bacterial colony. a) Full plasmid sequence with iFOXJ3 construct sequence highlighted in yellow. b) Part of the plasmid sequence visualised using online tool with iFOXJ3 construct sequence highlighted in blue. The highlighted sequence is GCCCCGAGCAGCCCCGAGAG which was similar to the sequence designed in Table 3.1 indicating successful sgRNA construct ligation into the plasmid.

4.4 Antibiotic selection

After transducing the 786-M1A CRISPRi cells with iFOXJ3 and sgNTC expression plasmids, the cells were treated with antibiotic to select for cells that had been positively transduced and harboured the respective plasmids. To recap, the plasmid pKLV-U6gRNA(BbsI)-PGKhygro2ABFP contained hygromycin resistance gene; therefore the positively transduced 786-M1A CRISPRi cells were selected using hygromycin, which the cells were resistant to. The cells were monitored over 5 days with visuals of the cells captured on day 0, 2 and 5 (**Figure 4.4**). As for cells in untransduced plate, all the cells were dead after treated with hygromycin.

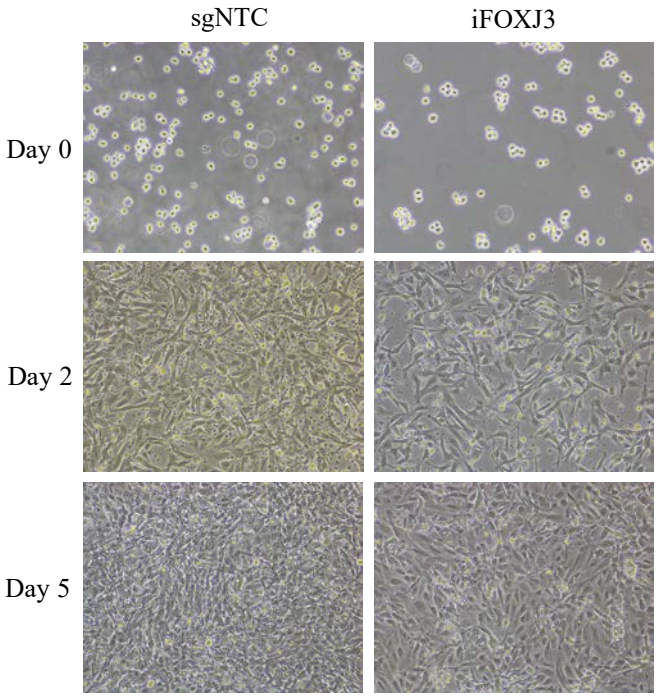

Figure 4.4: Antibiotic selection of 786-M1A CRISPRi cells for the iFOXJ3 and sgNTC with hygromycin. Both cell culture samples were transduced with lentiviral particle before selecting with antibiotic. The cells were monitored over 5 days and the growing cells were viewed under microscope on day 0, 2 and 5 (100X magnification). The cells were able to grow in the presence of hygromycin indicating successful transduction. Dead cells were also visible within the growing cells and were removed after selection process finished.

4.5 RNA extraction

The concentration and purity of RNA extracted from the 786-M1A cells were recorded and shown in **Table 4.1**. The RNA purity was measured through the absorbance ratio at 260/280 nm and 260/230 nm wavelengths. An A_{260}/A_{280} ratio of 1.8 – 2.2 and A_{260}/A_{230} ratio of 2.0 – 2.2 is considered as pure for RNA (Matlock, 2015). From the absorbance ratio of 260/280 nm, the RNA extracted were considered pure for all experimental repeats, with a good concentration yield. However, in repeats 2 and 3, the absorbance at 260/230 nm were low possibly due to residual TRIzol® reagents in the extracted RNA samples.

Table 4.1: The concentration and purity of RNA extracted from the 786-M1A CRISPRi cells. RNA purity was determined via the ratio at wavelength absorbance of 260/280 nm and 260/230 nm.

Experimental Repeat	Construct	Nucleic Acid Concentration, ng/µL	A_{260}/A_{280}	A_{260}/A_{230}
1	sgNTC	497.3	1.93	2.20
	iFOXJ3	251.9	1.93	1.74
2	sgNTC	1134.0	1.90	0.66
	iFOXJ3	188.9	1.72	0.29
3	sgNTC	112.7	1.68	0.52
	iFOXJ3	211.5	1.83	0.73

4.6 qPCR Analysis for *FOXJ3*-targeted kidney cancer cells

The C_t value (threshold cycle) was determined using the CFX Real-Time PCR Detection Systems (Bio-Rad) and then analysed using equations in **3.3.5** to calculate the normalized C_t value (ΔC_t) using *ACTB* as the reference gene. The relative gene expression ($-\Delta\Delta C_t$) was then calculated and the fold change ($2^{-\Delta\Delta Ct}$) measured. The resulting data were presented in a bar graph to illustrate the changes of gene expression in the control (sgNTC) and experimental condition (iFOXJ3) cells (**Figure 4.5**)

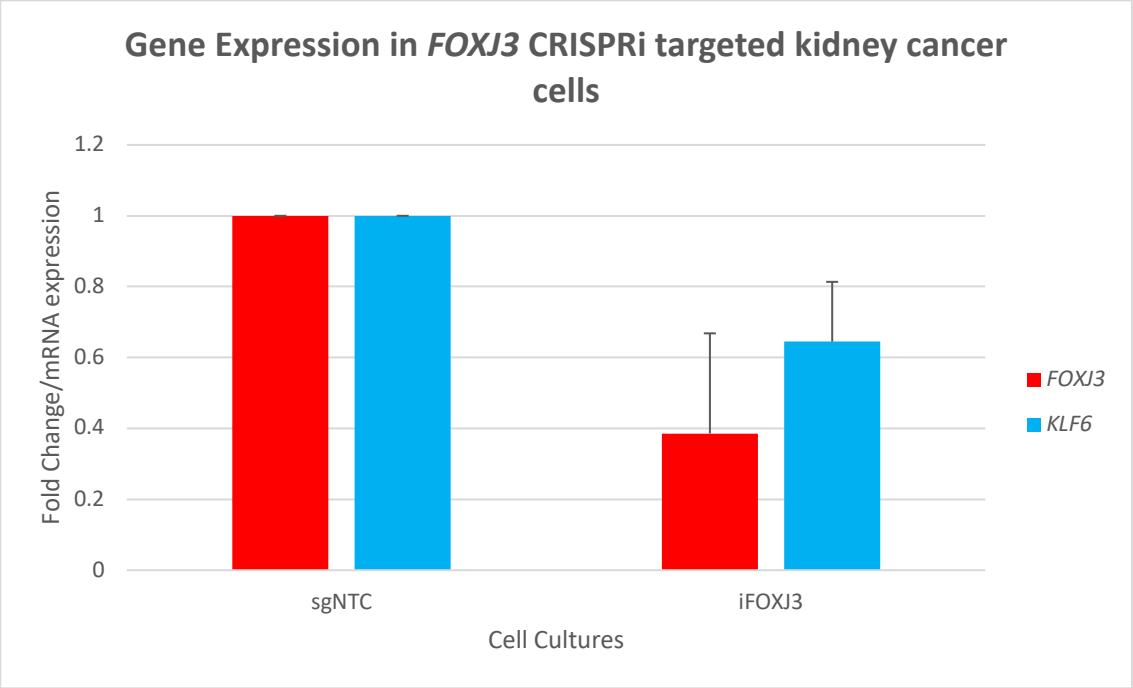

Figure 4.5: The change of gene expression in *FOXJ3* CRISPRi targeted cell (iFOXJ3) and control cell (sgNTC) samples. *FOXJ3* expression was reduced upon repression using CRISPRi. The iFOXJ3 cell samples also showed a reduction in *KLF6* gene expression. Average of three experiments. Error bars, standard deviation.

Based on **Figure 4.5**, the employed CRISPRi systems were successful in repressing *FOXJ3* expression in the 786-M1A CRISPRi cells. Three independent experimental repeats were performed and an average of 60% reduction in *FOXJ3* expression in iFOXJ3-transduced 786-M1A CRISPRi cells was observed, as compared to the sgNTC-transduced cells. This indicates the chosen iFOXJ3 construct was efficient in targeting *FOXJ3* Exon 1 and able to recruit dCas9-KRAB protein to this region that in turn inhibit the expression of *FOXJ3* in 786-M1A cells. Most importantly, reduction in *KLF6* expression in these *FOXJ3*-repressed 786-M1A CRISPRi cells was also observed. This observation was in line with the hypothesis that *FOXJ3* is a putative upstream transcriptional regulator of *KLF6* and binds to one of the *KLF6* super enhancer region in kidney cancer cells.

CHAPTER 5: DISCUSSION

The purpose of this study was to elucidate the role of *FOXJ3* in regulating the expression of super-enhancer associated *KLF6*. This in turn will allow us to gain a better understanding on the mechanism that regulate *KLF6* expression as *KLF6* has been shown to play central roles in modulating the hallmark features of ccRCC pathogenesis (Syafruddin et al., 2019). As discussed in Chapter 1, a strong super enhancer that is close to *KLF6* drives its expression (Syafruddin et al., 2019). This super enhancer locus drives *KLF6* expression in kidney cancer cells through a modular mechanism (Syafruddin et al., 2019). In a preliminary DNA binding motif search using Multiple Expectation Maximizations for Motif Elicitation (MEME) suite, *FOXJ3* was identified as one of the transcription factors that binds to one of the enhancer regions within *KLF6* super enhancer locus (Syafruddin, 2019) and hence potentially regulates *KLF6* expression in kidney cancer. Through the empirical research performed in this present study, it was found that *FOXJ3* repression using CRISPRi system caused a decreased *KLF6* expression (**Figure 4.5**), indicating that *FOXJ3* is a putative upstream transcriptional regulator of *KLF6*. This was in line with the hypothesis and objective of this study. This, however, needs further validation studies to confirm that *FOXJ3* does regulate *KLF6* expression in kidney cancer by binding to the *KLF6* super enhancer locus. In addition, these validation studies are critical to ensure that the observed downregulation of *KLF6* was indeed due to *FOXJ3* repression and not from off targets or other factors. To achieve this, one strategy that can be employed is to reintroduce exogenous *FOXJ3* into the CRISPRi-targeted *FOXJ3* 786-M1A cells and assess the expression of *FOXJ3* and *KLF6* in the *FOXJ3*-reintroduced cells. If *FOXJ3* expression is restored by the exogenous *FOXJ3,* the *KLF6* expression should theoretically be upregulated, which would further consolidate the hypothesis that *FOXJ3* is the upstream transcriptional regulator of *KLF6*. The author had attempted to

carry out this reintroduction experiment and managed to amplify the *FOXJ3* coding sequence (CDS) from the cDNA synthesised from the 786-M1A cells. However, due to time limitations and scope of this present study, the *FOXJ3* CDS cloning and subsequent reintroduction experiment would be pursued in-depth by the lab group in the future.

The data in this study can also be extended with two validation studies to confirm *FOXJ3* binding at the *KLF6* super enhancer region, namely *FOXJ3* ChIP-qPCR and luciferase reporter assay. Moreover, this study primarily looked at changes of gene expression in *FOXJ3* and *KLF6* after CRISPRi targeting. Thus, another area of observation in addition to changes of gene expression is to look at changes in cell growth and other molecular and phenotypic markers of ccRCC in iFOXJ3 and sgNTC cells. *KLF6* supports ccRCC growth *in vitro* by promoting the activation of important lipid metabolic regulators and enhancing lipid metabolism (Syafruddin et al., 2019), therefore the effect of *FOXJ3* repression may theoretically be observed with changes in lipid contents through *KLF6* downregulation. Whether *FOXJ3* plays a direct role in ccRCC cell growth are unknown at present. However, in a live-cell monitoring study done by Grant et al. (2012) , a *FOXJ3* knockdown caused a decrease in cell proliferation rate in human bone osteosarcoma epithelial cells (U2OS), indicating a role for *FOXJ3* in cell cycle control. Interestingly, the same study also identified the target genes for *FOXJ3*, in which it regulates a network of zinc finger proteins (Grant et al., 2012). Their findings fit with this research project in that *FOXJ3* regulates *KLF6* which belongs to the zinc finger family (Pearson et al., 2008).

As mentioned, attempts were made to reintroduced *FOXJ3* CDS into the *FOXJ3*-targeted cells. The cloning strategy for the reintroduction was to amplify *FOXJ3* coding sequence (CDS) from the cDNA of 786-M1A cells and clone the CDS into an expression

plasmid (**Figure 5.1**). Then, similar process of making lentiviral particle and transduction into 786-M1A cells to introduce the *FOXJ3* CDS into the cells would be employed. Finally, qPCR could be used to measure the changes in *FOXJ3* and *KLF6* expression in the *FOXJ3*-reintroduced cells. The challenges faced in this experiment was the optimization steps required for *FOXJ3* CDS amplification, which include optimizing the primers annealing temperature and concentration of cDNA template, as well as the purification of amplified *FOXJ3* CDS. Briefly, I managed to amplify the *FOXJ3* CDS where I obtained a clean band on the agarose gel that corresponded to the *FOXJ3* CDS reported size. However, I also obtained dirty and overlapping sequences when sending this amplified product for Sanger sequencing, indicating either there were multiple different amplicons with similar size (i.e., *FOXJ3* isoforms) or there was a problem with the purification steps. Therefore, as the study require much optimization and experimental scrutiny, the scope of this research project does not include this reintroduction experiment.

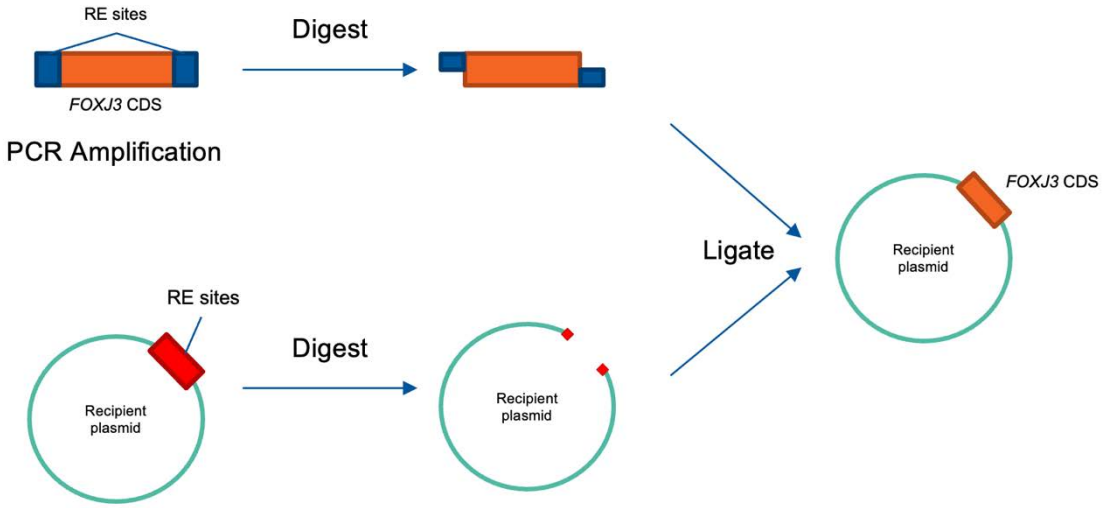

Figure 5.1: Molecular cloning strategy to reintroduce exogenous *FOXJ3* into 786-M1A cells. *FOXJ3* CDS can be PCR amplified with compatible restriction enzymes (RE) sites included. The gene insert and plasmid can then be digested using the REs and ligated before proceeding with bacterial transformation and cells transduction.

Taking a closer look at the sgRNA design for the CRISPRi system, the online tool predicted multiple possible sgRNA sequences, all of which targeted *FOXJ3* exon 1. As the objective of CRISPRi is to repress gene expression, the targeted sgRNAs were located near the transcription start site of the gene to allow the dCAS9-KRAB protein transcriptionally repress the gene near the start site or promoter region. As this study only employed one sgRNA out of the possible sequences, it may be worth repeating the experiment with multiple sgRNA sequences to compare *FOXJ3* repression, and statistical analysis can be done to evaluate the sgRNA efficiencies. Another note made during the study was that the bacterial colony on the negative control plate (**Figure 4.2**) had a couple of colonies formed that may occur from incomplete digestion or self-ligated plasmid (empty plasmid that contained no sgRNA). As the sequencing result from the plasmid extracted from the experimental bacterial colony plate showed the sgRNA insert within the plasmid (**Figure 4.3**), the bacterial transformation was considered a success.

In addition to CRISPRi, cloning and recombinant DNA technology, qPCR was the other main technique employed in this study. It was important to ensure that the RNA extracted for qPCR was of high quality and purity, as RNA with low purity may affect qPCR performance (Fleige & Pfaffl, 2006). The RNA extracted showed absorbance ratio at 260/280 nm wavelength as close to the pure value for RNA (**Table 4.1**), which is between 1.8 – 2.0 (Matlock, 2015). That said, only absorbance ratio was recorded which did not rule out issues with RNA integrity or genomic DNA contamination, of which are equally important for RNA work. The absorbance ratio for 260/230 nm were also showing probable organic compound residues in the extracted sample. However, as the study subsequently produced readable result, future repeat of similar work should employ methods to eliminate these possibilities. In effect, the gene expression analysis in this study is rendered as acceptable.

Based on the gene expression analysis, CRISPRi efficiencies can also be gauged. In all the experimental repeats, *FOXJ3* expression was lower than the control samples illustrated by the error bars on **Figure 4.5**. As the deviation were quite large, the efficiency of the CRISPRi system may have been influenced by other factors as *FOXJ3* repression were not always consistent. In future repeats, the cells may need to be extracted at a designated time point, for example when cells are at 90% confluency, to ensure that the *FOXJ3* expression was measured at the same time point as cell dynamics may play a role in influencing gene expression. This is also important to ensure the resulting *KLF6* expression level was measured accurately as cells may started to compensate with the loss of gene expression through other genes with overlapping function or expression pattern (El-Brolosy & Stainier, 2017).

Putting the data obtained into the context of *KLF6* gene expression, *FOXJ3* can now be categorized as one of the putative transcription factors that drives *KLF6* expression. As *KLF6* is driven by a super enhancer, many other transcription factors may need to be identified to understand how these transcription factors work together and drive their target gene. In the study by Syafruddin et al. (2019), one transcription factor that has been identified in regulating *KLF6* expression in ccRCC is hypoxia-inducible factor 2 alpha (HIF2A), which acts through binding at the super enhancer locus. As elaborated in Chapter 1, *VHL* inactivation that is associated with ccRCC leads to the accumulation of HIF2A (Syafruddin et al., 2019). This abundance of HIF2A in turn causes them to actively bind to the super enhancer region of *KLF6* and drive its expression, which may explain the high level of *KLF6* in ccRCC in comparison to normal kidney tissues (Syafruddin et al., 2019). *FOXJ3* may work in similar fashion, and its binding to the super enhancer region may be the key to understanding its mechanism in regulating *KLF6* expression. Another potential transcription factor that drives *KLF6* expression is the myocyte

enhancer factor 2 (MEF2) gene family which was identified as upstream transcriptional regulator of *KLF6* in some studies (Hashemi et al., 2015; Salma & McDermott, 2012). Salma and McDermott (2012) reported that MEF2-KLF6 pathway has a role in cell survival and apoptosis in the nervous system. In their study, *KLF6* was identified as the target gene for MEF2 family transcription factor, and loss of *KLF6* resulted in cell death in neuronal cells (Salma & McDermott, 2012). In addition, *KLF6* was also found as the target gene for MEF2 family transcription factor in cardiac muscle with similar role as an important pro-survival factor (Hashemi et al., 2015). More specifically, myocyte enhancer factor 2C (*MEF2C)* has been implicated as one of the genes that is involved in ccRCC pathogenesis (Yao et al., 2017). Therefore, in similar fashion to the strategy employed in this study, CRISPRi can be used to target *MEF2C* gene and assess its effect on *KLF6* expression. If there are repression in *KLF6* after *MEF2C* knockdown, this means that *MEF2C* is another transcriptional regulator of *KLF6* in addition to *HIF2A* and *FOXJ3*. Interestingly, as mentioned in passing in Chapter 1, previous studies have linked *FOXJ3* and *MEF2C* at which *Foxj3* transcriptionally activates *Mef2c* in skeletal muscle tissues (Alexander et al., 2010). Thus, another question worth pondering is whether *FOXJ3* also regulates *MEF2C* in ccRCC in addition to *KLF6*, or whether *FOXJ3* acts through *MEF2C* to drive *KLF6* expression in addition to its binding at the super enhancer region.

These questions were available only as the relationship between *FOXJ3* and *KLF6* have been established in this study. Although this study may benefit from further in-depth analysis, the preliminary data that provides a link between the *FOXJ3* and *KLF6* were invaluable to push the direction of *KLF6* gene expression study in the context of ccRCC pathogenesis. As it has been made clear that *KLF6* does not only depend on *FOXJ3*, many pieces of the super enhancer landscape puzzle are also needed to complete the picture.

Nevertheless, uncovering that *FOXJ3* as one of upstream transcriptional regulatory of *KLF6* has completed one part of the puzzle and opened many possible areas of research.

CHAPTER 6: CONCLUSION

This research project set out to determine whether *FOXJ3* binds to *KLF6* super enhancer locus and regulates the expression of this transcription factor in kidney cancer cells. In achieving this aim, CRISPRi was employed to target *FOXJ3* and repress its expression in 786-M1A cell line. The designed sgRNA was successfully ligated into an expression plasmid and transduced into the kidney cancer cell line, 786-M1A. The resulting downregulation of *FOXJ3* in 786-M1A CRISPRi cells indicate the success of the CRISPRi system. In turn, *KLF6* was also found to be downregulated, supporting the idea that *FOXJ3* is important for *KLF6* expression. This study in essence provides evidence for *FOXJ3* as one of the transcriptional regulators of *KLF6* and the data required to support further in-depth research into upstream regulation of *KLF6*. Circling back to the research aim, the resulting effect of downregulation of *FOXJ3* on *KLF6* together with the preliminary finding of *FOXJ3* DNA binding motif at the super enhancer region, the study concludes that *FOXJ3* regulates the expression of *KLF6* in kidney cancer cells.

Some suggestions to further interrogate the role of *FOXJ3* in regulating *KLF6* has also been proposed, for example reintroducing exogenous *FOXJ3* to rescue the expression of *FOXJ3* and *KLF6* in the CRISPRi targeted 786-M1A cells. Another research suggestion is to look at *MEF2C* as another transcriptional regulator of *KLF6*, as *MEF2C* has been shown to be closely linked with both *KLF6* (Hashemi et al., 2015; Salma & McDermott, 2012) and *FOXJ3* (Alexander et al., 2010). An intriguing prospect from these studies would be the development of a model for the mechanism of the super enhancers that drive *KLF6* expression, and ultimately identifying a viable therapeutic target within the super enhancer assembly for drug development.

REFERENCES

Alexander, M. S., Shi, X., Voelker, K. A., Grange, R. W., Garcia, J. A., Hammer, R. E., & Garry, D. J. (2010). Foxj3 transcriptionally activates Mef2c and regulates adult skeletal muscle fiber type identity. *Developmental Biology*, *337*(2), 396–404.

Ban, J. Y., Park, H. J., Kim, S. K., Kim, J. W., Lee, Y., Choi, I., Chung, J., & Hong, S. (2013). Association of forkhead box J3 (FOXJ3) polymorphisms with rheumatoid arthritis. *Molecular Medicine Reports*, *8*(4), 1235–1241.

Brodaczewska, K. K., Szczylik, C., Fiedorowicz, M., Porta, C., & Czarnecka, A. M. (2016). Choosing the right cell line for renal cell cancer research. *Molecular Cancer*, *15*, 1–15.

Cancer Genome Atlas Research Network. (2013). Comprehensive molecular characterization of clear cell renal cell carcinoma. *Nature*, *499*, 43–49.

Carlsson, P., & Mahlapuu, M. (2002). Forkhead transcription factors: key players in development and metabolism. *Developmental Biology*, *250*(1), 1–23.

Choueiri, T. K., Atkins, M. B., Bakouny, Z., Carlo, M. I., Drake, C. G., Jonasch, E., Kapur, P., Lewis, B., Linehan, W. M., Mitchell, M. J., Pal, S. K., Pels, K., Poteat, S., Rathmell, W. K., Rini, B. I., Signoretti, S., Tannir, N., Uzzo, R., Wood, C. G., & Hammers, H. J. (2021). Summary from the first Kidney Cancer Research Summit, September 12–13, 2019: A focus on translational research. *JNCI: Journal of the National Cancer Institute*, *113*(3), 234–243.

Choueiri, T. K., & Motzer, R. J. (2017). Systemic therapy for metastatic renal-cell carcinoma. *The New England Journal of Medicine*, *376*(4), 354–366.

Clark, D. J., Dhanasekaran, S. M., Petralia, F., Pan, J., Song, X., Hu, Y., da Veiga Leprevost, F., Reva, B., Lih, T. S. M., Chang, H. Y., Ma, W., Huang, C., Ricketts, C. J., Chen, L., Krek, A., Li, Y., Rykunov, D., Li, Q. K., Chen, L. S., … Zhang, H. (2019). Integrated proteogenomic characterization of clear cell renal cell carcinoma. *Cell*, *179*, 964–983.

Delmore, J. E., Issa, G. C., Lemieux, M. E., Rahl, P. B., Shi, J., Jacobs, H. M., Kastritis, E., Gilpatrick, T., Paranal, R. M., Qi, J., Chesi, M., Schinzel, A. C., McKeown, M. R., Heffernan, T. P., Vakoc, C. R., Bergsagel, P. L., Ghobrial, I. M., Richardson, P. G., Young, R. A., … Mitsiades, C. S. (2011). BET bromodomain inhibition as a therapeutic strategy to target c-Myc. *Cell*, *146*(6), 904–917.

DiFeo, A., Martignetti, J., & Narla, G. (2009). The role of KLF6 and its splice variants in cancer therapy. *Drug Resistance Updates : Reviews and Commentaries in Antimicrobial and Anticancer Chemotherapy*, *12*(1–2), 1–7.

El-Brolosy, M. A., & Stainier, D. Y. R. (2017). Genetic compensation: A phenomenon in search of mechanisms. *PLoS Genetics*, *13*(7), Article#e1006780.

Fleige, S., & Pfaffl, M. W. (2006). RNA integrity and the effect on the real-time qRT-PCR performance. *Molecular Aspects of Medicine*, *27*, 126–139.

Furlong, E. E. M., & Levine, M. (2018). Developmental enhancers and chromosome topology. *Science*, *361*(6409), 1341–1345.

Grant, G. D., Gamsby, J., Martyanov, V., Brooks, L., George, L. K., Mahoney, J. M., Loros, J. J., Dunlap, J. C., & Whitfield, M. L. (2012). Live-cell monitoring of periodic gene expression in synchronous human cells identifies Forkhead genes involved in cell cycle control. *Molecular Biology of the Cell*, *23*(16), 3079–3093.

Habuka, M., Fagerberg, L., Hallström, B. M., Kampf, C., Edlund, K., Sivertsson, A., Yamamoto, T., Pontén, F., Uhlén, M., & Odeberg, J. (2014). The Kidney transcriptome and proteome defined by transcriptomics and antibody-based profiling. *PLoS ONE*, *9*(12), Article#e116125.

Hashemi, S., Salma, J., Wales, S., & McDermott, J. C. (2015). Pro-survival function of MEF2 in cardiomyocytes is enhanced by β-blockers. *Cell Death Discovery*, *1*(1), 1–11.

Hnisz, D., Abraham, B. J., Lee, T. I., Lau, A., Saint-André, V., Sigova, A. A., Hoke, H. A., & Young, R. A. (2013). Super-enhancers in the control of cell identity and disease. *Cell*, *155*(4), 934–947.

Hsieh, J. J., Purdue, M. P., Signoretti, S., Swanton, C., Albiges, L., Schmidinger, M., Heng, D. Y., Larkin, J., & Ficarra, V. (2017). Renal cell carcinoma. *Nature Reviews Disease Primers*, *3*(1), 1–19.

Jia, Z., Wan, F., Zhu, Y., Shi, G., Zhang, H., Dai, B., & Ye, D. (2018). Forkhead-box series expression network is associated with outcome of clear-cell renal cell carcinoma. *Oncology Letters*, *15*(6), Article#8680.

Jin, J., Zhou, S., Li, C., Xu, R., Zu, L., You, J., & Zhang, B. (2014). MiR-517a-3p accelerates lung cancer cell proliferation and invasion through inhibiting FOXJ3 expression. *Life Sciences*, *108*(1), 48–53.

Jung, M., Ramankulov, A., Roigas, J., Johannsen, M., Ringsdorf, M., Kristiansen, G., & Jung, K. (2007). In search of suitable reference genes for gene expression studies of human renal cell carcinoma by real-time PCR. *BMC Molecular Biology*, *8*, Article#47.

Koike-Yusa, H., Li, Y., Tan, E. P., Velasco-Herrera, M. D. C., & Yusa, K. (2014). Genome-wide recessive genetic screening in mammalian cells with a lentiviral CRISPR-guide RNA library. *Nature Biotechnology*, *32*(3), 267–273.

Krijger, P. H. L., & de Laat, W. (2016). Regulation of disease-associated gene expression in the 3D genome. *Nature Reviews Molecular Cell Biology*, *17*(12), 771–782.

Landgren, H., & Carlsson, P. (2004). Foxj3, a novel mammalian forkhead gene expressed in neuroectoderm, neural crest, and myotome. *Developmental Dynamics*, *231*(2), 396–401.

Livak, K. J., & Schmittgen, T. D. (2001). Analysis of relative gene expression data using real-time quantitative PCR and the 2(-Delta Delta C(T)) Method. *Methods*, *25*(4), 402–408.

Matlock, B. (2015). Assessment of nucleic acid purity. In *Thermo Fisher Scientific*. www.thermoscientific.com

Matsumoto, N., Kubo, A., Liu, H., Akita, K., Laub, F., Ramirez, F., Keller, G., & Friedman, S. L. (2006). Developmental regulation of yolk sac hematopoiesis by Krüppel-like factor 6. *Blood*, *107*(4), Article#1365.

Motzer, R. J., Hutson, T. E., McCann, L., Deen, K., & Choueiri, T. K. (2014). Overall survival in renal-cell carcinoma with pazopanib versus sunitinib. *The New England Journal of Medicine*, *370*(18), 1769–1770.

Pantuck, A., Seligson, D., Klatte, T., Yu, H., Leppert, J., Moore, L., O'Toole, T., Gibbons, J., Belldegrun, A., & Figlin, R. (2007). Prognostic relevance of the mTOR pathway in renal cell carcinoma: implications for molecular patient selection for targeted therapy. *Cancer*, *109*(11), 2257–2267.

Pearson, R., Fleetwood, J., Eaton, S., Crossley, M., & Bao, S. (2008). Krüppel-like transcription factors: A functional family. *The International Journal of Biochemistry & Cell Biology*, *40*(10), 1996–2001.

Pollak, N. M., Hoffman, M., Goldberg, I. J., & Drosatos, K. (2018). Krüppel-like factors: Crippling and un-crippling metabolic pathways. *JACC: Basic to Translational Science*, *3*(1), 132–156.

Roadmap Epigenomics Consortium, Kundaje, A., Meuleman, W., Ernst, J., Bilenky, M., Yen, A., Heravi-Moussavi, A., Kheradpour, P., Zhang, Z., Wang, J., Ziller, M. J., Amin, V., Whitaker, J. W., Schultz, M. D., Ward, L. D., Sarkar, A., Quon, G., Sandstrom, R. S., Eaton, M. L., … Kellis, M. (2015). Integrative analysis of 111 reference human epigenomes. *Nature*, *518*, 317–330.

Robb, V., Karbowniczek, M., Klein-Szanto, A., & Henske, E. (2007). Activation of the mTOR signaling pathway in renal clear cell carcinoma. *The Journal of Urology*, *177*(1), 346–352.

Rocha, A. M. A. de la, González-Huarriz, M., Guruceaga, E., Mihelson, N., Tejada-Solís, S., Díez-Valle, R., Martínez-Vélez, N., Fueyo, J., Gomez-Manzano, C., Alonso, M. M., Laterra, J., & López-Bertoni, H. (2020). miR-425-5p, a SOX2 target, regulates the expression of FOXJ3 and RAB31 and promotes the survival of GSCs. *Archives of Clinical and Biomedical Research*, *4*(3), Article#238.

Sabatini, D. M. (2006). mTOR and cancer: insights into a complex relationship. *Nature Reviews Cancer*, *6*, 729–734.

Salma, J., & McDermott, J. C. (2012). Suppression of a MEF2-KLF6 survival pathway by PKA signaling promotes apoptosis in embryonic hippocampal neurons. *Journal of Neuroscience*, *32*(8), 2790–2803.

Sengupta, S., & George, R. E. (2017). Super-enhancer-driven transcriptional dependencies in cancer. *Trends in Cancer*, *3*(4), 269–281.

Siegel, R. L., Miller, K. D., & Jemal, A. (2018). Cancer statistics, 2018. *CA: A Cancer Journal for Clinicians*, *68*(1), 7–30.

Simeoni, F., Romero-Camarero, I., Camera, F., Amaral, F. M. R., Sinclair, O. J., Papachristou, E. K., Spencer, G. J., Lie-A-Ling, M., Lacaud, G., Wiseman, D. H., Carroll, J. S., & Somervaille, T. C. P. (2021). Enhancer recruitment of transcription repressors RUNX1 and TLE3 by mis-expressed FOXC1 blocks differentiation in acute myeloid leukemia. *Cell Reports*, *36*(12), Article#109725.

Spielmann, M., Lupiáñez, D. G., & Mundlos, S. (2018). Structural variation in the 3D genome. *Nature Reviews Genetics*, *19*(7), 453–467.

Syafruddin, S. E. (2019). A KLF6-driven transcriptional network links lipid homeostasis and tumour growth in clear cell renal cell carcinoma (Doctoral thesis). Retrieved from https://www.repository.cam.ac.uk/handle/1810/294470

Syafruddin, S. E., Rodrigues, P., Vojtasova, E., Patel, S. A., Zaini, M. N., Burge, J., Warren, A. Y., Stewart, G. D., Eisen, T., Bihary, D., Samarajiwa, S. A., & Vanharanta, S. (2019). A KLF6-driven transcriptional network links lipid homeostasis and tumour growth in renal carcinoma. *Nature Communications*, *10*(1), 1–13.

Tang, F., Yang, Z., Tan, Y., & Li, Y. (2020). Super-enhancer function and its application in cancer targeted therapy. *Npj Precision Oncology*, *4*(2), 1–7.

Tetreault, M.-P., Yang, Y., & Katz, J. P. (2013). Krüppel-like factors in cancer. *Nature Reviews Cancer*, *13*, 701–713.

Thandapani, P. (2019). Super-enhancers in cancer. *Pharmacology & Therapeutics*, *199*, 129–138.

The ENCODE Project Consortium, Dunham, I., Kundaje, A., Aldred, S. F., Collins, P. J., Davis, C. A., Doyle, F., Epstein, C. B., Frietze, S., Harrow, J., Kaul, R., Khatun, J., Lajoie, B. R., Landt, S. G., Lee, B. K., Pauli, F., Rosenbloom, K. R., Sabo, P., Safi, A., … Lochovsky, L. (2012). An integrated encyclopedia of DNA elements in the human genome. *Nature*, *489*, 57–74.

Uhlen, M., Zhang, C., Lee, S., Sjöstedt, E., Fagerberg, L., Bidkhori, G., Benfeitas, R., Arif, M., Liu, Z., Edfors, F., Sanli, K., von Feilitzen, K., Oksvold, P., Lundberg, E., Hober, S., Nilsson, P., Mattsson, J., Schwenk, J. M., Brunnström, H., … Ponten, F. (2017). A pathology atlas of the human cancer transcriptome. *Science*, *357*(6352).

Vanharanta, S., Shu, W., Brenet, F., Ari Hakimi, A., Heguy, A., Viale, A., Reuter, V. E., Hsieh, J. J. D., Scandura, J. M., & Massagué, J. (2012). Epigenetic expansion of VHL-HIF signal output drives multiorgan metastasis in renal cancer. *Nature Medicine*, *19*(1), 50–56.

Whyte, W. A., Orlando, D. A., Hnisz, D., Abraham, B. J., Lin, C. Y., Kagey, M. H., Rahl, P. B., Lee, T. I., & Young, R. A. (2013). Master transcriptionfFactors and mediator establish super-enhancers at key cell identity genes. *Cell*, *153*(2), Article#319.

Wolf, M. M., Kimryn Rathmell, W., & Beckermann, K. E. (2020). Modeling clear cell renal cell carcinoma and therapeutic implications. *Oncogene*, *39*(17), Article#3426.

Yao, X., Tan, J., Lim, K. J., Koh, J., Ooi, W. F., Li, Z., Huang, D., Xing, M., Chan, Y. S., Qu, J. Z., Tay, S. T., Wijaya, G., Lam, Y. N., Hong, J. H., Lee-Lim, A. P., Guan, P., Ng, M. S. W., He, C. Z., Lin, J. S., … Tan, P. (2017). VHL deficiency drives enhancer activation of oncogenes in clear cell renal cell carcinoma. *Cancer Discovery*, *7*(11), 1284–1305.

Zhang, J. Y., Su, X. P., Li, Y. N., & Guo, Y. H. (2019). MicroRNA-425-5p promotes the development of prostate cancer via targeting forkhead box J3. *European Review for Medical and Pharmacological Sciences*, *23*(2), 547–554.

Zuber, J., Shi, J., Wang, E., Rappaport, A. R., Herrmann, H., Sison, E. A., Magoon, D., Qi, J., Blatt, K., Wunderlich, M., Taylor, M. J., Johns, C., Chicas, A., Mulloy, J. C., Kogan, S. C., Brown, P., Valent, P., Bradner, J. E., Lowe, S. W., & Vakoc, C. R. (2011). RNAi screen identifies Brd4 as a therapeutic target in acute myeloid leukaemia. *Nature*, *478*(7370), 524–528.